

## Characterization of the *In Situ* Structural and Interfacial Properties of the Cationic Hydrophobic Heteropolypeptide, KL<sub>4</sub>, in Lung Surfactant Bilayer and Monolayer Models at the Air–Water Interface: Implications for Pulmonary Surfactant Delivery

Heidi M. Mansour,<sup>\*,†</sup> Srinivasan Damodaran,<sup>‡</sup> and George Zografi<sup>†</sup>

*Division of Pharmaceutical Sciences, School of Pharmacy, University of Wisconsin–Madison, Madison, Wisconsin 53705, and Department of Food Science, University of Wisconsin–Madison, Madison, Wisconsin 53706*

Received September 12, 2007; Revised Manuscript Received May 12, 2008; Accepted May 27, 2008

**Abstract:** This study examines the various equilibrium *in situ* secondary structures of the pharmaceutical heteropolypeptide, KL<sub>4</sub>, in the solid state, in solution, and in the monolayer state alone and mixed with dipalmitoylphosphatidylcholine (DPPC) and palmitoyloleoylphosphatidylglycerol (POPG). *In situ* surface circular dichroism spectroscopy, using a method first reported by Damodaran (Damodaran, S. *Anal. Bioanal. Chem.* **2003**, 376, 182–188), of equilibrated KL<sub>4</sub>, DPPC/KL<sub>4</sub>, POPG/KL<sub>4</sub>, and DPPC/POPG/KL<sub>4</sub> monolayers at the air–water interface was used to examine the *in situ* two-dimensional conformation of KL<sub>4</sub>. Gravimetric vapor sorption by solid KL<sub>4</sub> was used to analyze the effects of water molecules on the conformation of KL<sub>4</sub> when confined as a monolayer at the surface of water. Solid-state KL<sub>4</sub> conformation was determined by X-ray powder diffraction (XRPD). The equilibrium interfacial and spreading properties were measured at 25 °C, 37 °C, and 45 °C using the Wilhelmy plate method and Langmuir film balance. Equilibrium phase transition temperatures were measured using differential scanning calorimetry (DSC). It was found that solid-state KL<sub>4</sub>, which takes up very little water, exhibits  $\beta$ -sheet and  $\alpha$ -helix secondary structures, whereas KL<sub>4</sub> in solution appears to exist only as an  $\alpha$ -helix. KL<sub>4</sub> forms a stable, insoluble monolayer, exhibiting  $\beta$ -sheet and aperiodic structures. These structures provide KL<sub>4</sub>, when confined in two-dimensions, the structural flexibility to maximize favorable cationic lysine–water interactions and favorable leucine–leucine hydrophobic and van der Waals interactions; while effectively “shielding” the leucine residues away from water. In DPPC/KL<sub>4</sub> monolayers, KL<sub>4</sub> retains its native  $\beta$ -sheet and aperiodic structures, consistent with phase separation of DPPC and KL<sub>4</sub> in bilayers and monolayers. In POPG/KL<sub>4</sub> monolayers, KL<sub>4</sub> exhibits an increase in aperiodic secondary structures (loss of  $\beta$ -sheet) to maximize favorable electrostatic interactions, consistent with the observed negative deviations from ideal monolayer mixing.

**Keywords:** biomacromolecule conformation/secondary structure; phospholipids; water vapor absorption/hydration; solid-state; Langmuir films; phase transitions; molecular interactions; surface structure; *in situ* surface circular dichroism; bilayer–monolayer equilibria

### Introduction

Dipalmitoylphosphatidylcholine (DPPC) is the primary phospholipid component in lung surfactant, making up

55–60% of the zwitterionic phosphatidylcholine (PC) lipid.<sup>1,2</sup> This DPPC-rich monolayer is capable of lowering the surface tension to very low levels and maintaining lung stability.<sup>3–5</sup> However, other components, both phospholipids and proteins, are present to overcome the intrinsic deficiency of DPPC to

\* To whom correspondence should be addressed. Mailing address: University of North Carolina–Chapel Hill, School of Pharmacy, Division of Molecular Pharmaceutics, 311 Pharmacy Lane, 1311 Kerr Hall-Dispersed Systems Laboratory, Chapel Hill, NC 27599-7360. E-mail: hmmansour@unc.edu. Tel: (919) 966-0484. Fax: (919) 966-0197.

<sup>†</sup> School of Pharmacy, University of Wisconsin–Madison.

<sup>‡</sup> Department of Food Science, University of Wisconsin–Madison.

- (1) van Golde, L. M. G.; Batenburg, J.; Robertson, B. The Pulmonary Surfactant System: Biochemical Aspects and Functional Significance. *Phys. Rev.* **1988**, 68, 374–455.
- (2) Batenburg, J. Biosynthesis, Secretion, and Recycling of Surfactant Components. In *Lung Biology in Health and Disease*; Lenfant, C. Ed.; Marcel Dekker: New York, 1995; pp 47–73.

significantly and maximally spread from the bilayer state at 37 °C onto an aqueous surface.<sup>6</sup> Such materials, that readily spread themselves, act to fluidize the monolayer and promote the spreading of DPPC.<sup>6–9</sup> It is this highly condensed nature of the DPPC monolayer, however, that appears to provide the extraordinarily low surface tensions at high levels of compression. At these high levels of monolayer compression, fluidizers, such as phosphatidylglycerol (PG), therefore, must be removed, in some way after initially promoting the spreading of DPPC, to allow for the formation of condensed tightly packed DPPC regions in the resulting highly compressed monolayer.<sup>10</sup>

“KL<sub>4</sub>” is a 21-amino acid cationic hydrophobic heteropolypeptide composed of the amino acids lysine (K) and leucine (L) in four repeating KL motifs followed by K and having a primary sequence of (KL<sub>4</sub>)<sub>4</sub>K. KL<sub>4</sub> has been shown to be very effective in the clinical treatment of animal and human RDS (respiratory distress syndrome) and ARDS (adult respiratory distress syndrome).<sup>11,12</sup> KL<sub>4</sub> is currently available on the pharmaceutical market as one of the active components in the new-generation, first completely synthetic non-immunogenic, lung surfactant replacement product Surfaxin (lucinactant), administered in the solid-state as a dry power that is reconstituted prior to use. Some controversy as to the exact mechanism, orientation, and site of action of KL<sub>4</sub> in

bilayers and monolayers still exists.<sup>13,14</sup> The orientation of KL<sub>4</sub> in a monolayer and bilayer to date has not been established under thermodynamic equilibrium conditions, and the monolayer model for the interfacial structure of KL<sub>4</sub> is partly based on limited bilayer data.<sup>15</sup> While infrared reflection–absorption spectroscopy (IRRAS) has been reported<sup>16</sup> in probing the structure of KL<sub>4</sub> in select phospholipid monolayer systems *in situ*, it is noted that these select monolayer systems on a D<sub>2</sub>O subphase were acquired under dynamic, time-dependent conditions, which can significantly affect surface conformational structure,<sup>17,18</sup> surface properties,<sup>17,18</sup> the surface phase transitions,<sup>6</sup> and the surface collapse pressure<sup>6</sup> of monolayers and surface-active polypeptides, which may not necessarily relate to the physiological conditions in the lung. Equilibrium measurements, as a start, would delineate and clarify our understanding of the interactions among the components, including interfacial and conformational structural properties, which are fundamental to the function of lung surfactant and any effective lung surfactant replacement drug product.

It has been suggested that, for monolayers containing a ternary mixture of DPPC/POPG/KL<sub>4</sub>, cationic KL<sub>4</sub> interacts electrostatically with anionic palmitoylphosphatidylglycerol (POPG) and not with zwitterionic DPPC. This specific electrostatic interaction between KL<sub>4</sub> and POPG increases the ability of the bilayer to spread to a maximum equilibrium spreading pressure and achieves the maximum equilibrium collapse pressure of the monolayer (monolayer condensation) through enhanced surface phase separation of DPPC and POPG.<sup>10</sup> In nature, protein activity is optimized by uniquely folded conformations, which are crucial for biological activity. A central aspect of the molecular biophysics of proteins and peptides is the relationship between functionality and folding. Therefore, information about the structure can, in turn, be valuable information in understanding function. Investigating the changes of proteins and peptides structures at the air–water interface in the past has been done by first transferring the monolayer onto a quartz plate and then analyzing the protein film by CD or

- (3) Schurch, S.; Goerke, J.; Clements, J. A. Determination of surface tension in the lung. *Proc. Natl. Acad. Sci. U.S.A.* **1976**, *73*, 4698–4702.
- (4) Clements, J. A.; Hustead, R. F.; Johnson, R. P.; Gribetz, I. Pulmonary surface tension and alveolar stability. *J. Appl. Physiol.* **1961**, *16*, 444–450.
- (5) Keough, K. Lipid Fluidity and Respiratory Distress Syndrome. In *Membrane Fluidity in Biology*; Aloia, R., Boggs, T. Eds.; Academic Press: New York, 1985; pp 40–78.
- (6) Mansour, H. M.; Zografi, G. Relationships between Equilibrium Spreading Pressure and Phase Equilibria of Phospholipid Bilayers and Monolayers at the Air–Water Interface. *Langmuir* **2007**, *23*, 3809–3819.
- (7) Koppenol, S.; Yu, H.; Zografi, G. Mixing of Saturated and Unsaturated Phosphatidylcholines and Phosphatidylglycerols in Monolayers at the Air/ Water Interface. *J. Colloid Interface Sci.* **1997**, *189*, 158–166.
- (8) Mansour, H.; Wang, D.-S.; Chen, C.-S.; Zografi, G. Comparison of Bilayer and Monolayer Properties of Phospholipid Systems Containing Dipalmitoylphosphatidylglycerol and Dipalmitoylphosphatidylinositol. *Langmuir* **2001**, *17*, 6622–6632.
- (9) Mansour, H. M.; Zografi, G. Relationships between Bilayer–Monolayer Equilibria and Thermotropic Phase Behavior of Phospholipid Mixtures containing Dipalmitoylphosphatidylcholine at the Air–Water Interface. *J. Colloid Interface Sci.*, submitted.
- (10) Ma, J.; Koppenol, S.; Yu, H.; Zografi, G. Effects of a Cationic and Hydrophobic Peptide, KL<sub>4</sub>, on Model Lung Surfactant Lipid Monolayers. *Biophys. J.* **1998**, *74*, 1899–1907.
- (11) Cochrane, C.; Revak, S.; Merritt, T.; Heldt, G.; Hallman, M.; Cunningham, M.; et al. The Efficacy and Safety of KL<sub>4</sub>-Surfactant in Preterm Infants with Respiratory Distress Syndrome. *Am. J. Respir. Crit. Care Med.* **1996**, *153*, 404–410.
- (12) Wiswell, T. E.; Smith, R. M.; Katz, L. B.; Mastroianni, L.; Wong, D. Y.; Sillms, D.; et al. Bronchopulmonary segmental lavage with surfaxin (KL<sub>4</sub>-surfactant) for acute respiratory distress syndrome. *Am. J. Respir. Crit. Care Med.* **1999**, *160*, 1188–1195.

- (13) Cochrane, C. Surfactant protein B and mimic peptides in the function of pulmonary surfactant. *FEBS Lett.* **1998**, *430*, 424.
- (14) Gustafsson, M.; Vandenbussche, G.; Curstedt, T.; Ruysschaert, J.; Johansson, J. The 21-residue surfactant peptide (LysLeu<sub>4</sub>)<sub>4</sub>Lys(KL<sub>4</sub>) is a transmembrane  $\alpha$ -helix with a mixed nonpolar/polar surface. *FEBS Lett.* **1996**, *384*, 185–188.
- (15) Gustafsson, M.; Vandenbussche, G.; Curstedt, T.; Ruysschaert, J.; Johansson, J. Answer. *FEBS Lett.* **1998**, *430*, 425.
- (16) Cai, P.; Flach, C. R.; Mendelsohn, R. An infrared reflection-absorption study of the secondary structure in (KL<sub>4</sub>)<sub>4</sub>K, a therapeutic agent for respiratory distress syndrome in aqueous monolayers with phospholipids. *Biochemistry* **2003**, *42*, 9446–9452.
- (17) Bender, M. Interfacial Phenomena in Biological Systems. In *Interfacial Phenomena in Biological Systems*, 1st ed.; Bender, M. Ed.; Marcel Dekker, Inc.: New York, 1991.
- (18) Norde, W. *Colloids and Interfaces in Life Sciences*, 1st ed.; Marcel Dekker, Inc.: New York, 2003.

Fourier-transformed infrared (FTIR) spectroscopy.<sup>19,20</sup> Increasing  $\beta$ -sheet structures in monolayers has been shown *in situ* for non-lung surfactant protein systems under different conditions using sum frequency generation vibrational spectroscopy.<sup>21</sup> Because the conformation of the peptide or protein in the monolayer film on a solid surface may not be the same as it would have been at the air–liquid interface, a noninvasive *in situ* circular dichroism method to probe the secondary structure at the air–water interface has been developed by Damodaran.<sup>22</sup> For water-soluble proteins in aqueous solution, changes in secondary structure on transfer from the solution to the air–water interface follow a general trend of decreasing  $\alpha$ -helix and increasing  $\beta$ -sheet and aperiodic structures.<sup>22</sup>

In this study, we report for the first time and evaluate the following, all under equilibrium time-independent conditions that allow us to begin to decipher the molecular interactions and *in situ* conformational structures in three dimensions (bulk) and when confined to an interface, using *in situ* surface circular dichroism spectroscopy: (1) the thermal, structural, hydration and surface-active properties of the synthetic cationic hydrophobic heteropolypeptide, KL<sub>4</sub>, alone and in the presence of a rational selection of phospholipids in bilayer and monolayer lung surfactant models at the air–water interface; (2) the molecular interactions of KL<sub>4</sub> with phospholipid bilayer and monolayer lung surfactant models, in the context of bilayer and monolayer phase behavior under equilibrium conditions; (3) the three-dimensional and two-dimensional structural characterization of KL<sub>4</sub> *in situ* alone and in the presence of these rationally selected phospholipids. The surface chemical implications for pulmonary surfactant delivery are then discussed.

## Experimental Methods

**Materials. (a) Phospholipids.** The following synthetic phospholipids were obtained from Avanti Polar Lipids, Inc. (Alabaster, AL), with a stated purity of >99+%, and were used as received: 1,2-dipalmitoyl-*sn*-glycero-3-phosphocholine (DPPC), 1-palmitoyl-2-oleoyl-*sn*-3-phospho-*rac*-glycerol sodium salt (POPG), and 1-palmitoyl-2-{12-[(7-nitro-2-1,3-benzoxadiazol-4-yl)amino]dodecanoyl}-*sn*-glycero-3-phosphocholine (NBD-PC). All phospholipid powder samples were stored in an ultralow temperature laboratory freezer (Revco Elite, Revco Scientific, Inc., Asheville, NC) at  $-73^{\circ}\text{C}$ .

**(b) “KL<sub>4</sub>”.** Solid-state synthesis of KL<sub>4</sub> with the primary sequence of (KL<sub>4</sub>)<sub>4</sub>K was carried out according to the reported method.<sup>23,24</sup> Due to its surface activity, KL<sub>4</sub> has a strong tendency to gel in aqueous solution or in ethanol, which limited high purification in large quantities by standard purification methods. Following the synthesis, therefore, the peptide-resin was rinsed with dichloromethane, dried, and then cleaved and deprotected (removal of Boc from lysine) by reacting with trifluoroacetic acid (TFA) containing 5% water for 2 h. The solution was then filtered, sedimented by centrifugation, and washed twice with ether to extract residual TFA. The precipitate was vacuum-dried, dissolved in water: acetonitrile:acetic acid (50:40:10), and lyophilized (additional purification step). The lyophilized peptide was dissolved a second time (60:40 water:acetonitrile containing 0.1% TFA or in 50% acetic acid), and then 0.5% of the peptide solution was removed for analytical high-pressure liquid chromatography (HPLC) and mass spectroscopy which conformed to the molecular weight of KL<sub>4</sub> (MS, 2470.2 molecular weight). Final chromatographic purity was 99% after purification using chromatography on a preparative scale C-18 column. Freeze-drying was carried out to produce the final product, which was stored at  $-73^{\circ}\text{C}$ .

The water used in all experiments was house-distilled water passed through a 5-cartridge Barnstead PCS water purification system with a resistivity of 18 M $\Omega$ -cm. This was then twice-distilled from an alkaline permanganate solution and from dilute sulfuric acid and collected in a glass container. All samples containing phospholipid were stored for no more than three months at  $-21^{\circ}\text{C}$ . Chloroform and methanol were the organic solvents utilized for the various monolayer spreading experiments and were obtained from Sigma-Aldrich in 99.93% ACS HPLC grade (Sigma Aldrich Company, Inc., Milwaukee, WI). Tris, ultrapure hydroxymethylaminomethane, 99.9% (United States Biochemical Co.), and sodium chloride, 99.999% (Sigma-Aldrich), were used as received. The solvent used in DPPC and POPG monolayer studies was chloroform. KL<sub>4</sub> was dissolved in a ternary solvent mixture of chloroform:methanol:ultrapure triply distilled water.

**Methods. (a) Main Bilayer Gel-to-Liquid Crystalline Phase Transition Temperature,  $T_m$ , Measurements Using Differential Scanning Calorimetry (DSC).** The method used was described earlier.<sup>6,8,9,25</sup> The equilibrium  $T_m$  values of fully hydrated phospholipids (15% w/w) containing pH 7.40 150 mM NaCl 10 mM TRIS ultrapure buffer were measured at a heating rate of 1.0  $^{\circ}\text{C}/\text{minute}$  using

- (19) Briggs, M. S.; Cornell, D. G.; Dluhy, R. A.; Gierasch, L. M. Conformations of signal peptides induced by lipids suggest initial steps in protein export. *Science* **1986**, 233, 206–208.
- (20) Cornell, D. G. Circular Dichroism of polypeptide monolayers. *J. Colloid Interface Sci.* **1979**, 70, 167–180.
- (21) Wang, J.; Chen, X. Y.; Clarke, M. L.; Chen, Z. Detection of chiral sum frequency generation vibrational spectra of proteins and peptides at interfaces *in situ*. *Proc. Natl. Acad. Sci. U.S.A.* **2005**, 102, 4978–4983.
- (22) Damodaran, S. *In situ* measurement of conformational changes in proteins at liquid interfaces by circular dichroism spectroscopy. *Anal. Bioanal. Chem.* **2003**, 376, 182–188.

- (23) Revak, S. D.; Merritt, T. A.; Hallman, M.; Heldt, G.; La Polla, R. J.; Hoey, K.; et al. The use of synthetic peptides in the formation of biophysically active pulmonary surfactants. *Pediatr. Res.* **1991**, 29, 460–465.
- (24) Cochrane, C. G.; Revak, S. D. Pulmonary Surfactant Protein B (SP-B): Structure-Function Relationships. *Science* **1991**, 254, 566–568.
- (25) Mansour, H. M.; Zografi, G. The relationship between water vapor absorption and desorption by phospholipids and bilayer phase transitions. *J. Pharm. Sci.* **2007**, 96, 377–396.



a Seiko SSC 220C DSC (Seiko Instruments, Horsham, PA). In order to maintain the level of hydration, the aluminum Seiko DSC pans were hermetically sealed.

**(b) Measurement of Bilayer Equilibrium Spreading Pressure,  $\pi_e$ .** Powder was deposited directly onto the surface<sup>6,8,9</sup> to measure  $\pi_e$ . Final  $\pi_e$  values were determined when the change in the surface pressure of the monolayer was less than 0.2 mN/h, independent of the amount of excess bulk lipid material on the surface and independent of the total surface area upon which the monolayer was spread. As reported earlier,<sup>6,8,9</sup> studies were carried out at 25 °C, 37 °C, and 45 °C.

**(c) Monolayer Equilibrium Surface Pressure—Area,  $\pi$ —A, Isotherm Measurements.** The Wilhelmy plate method and Langmuir film balance were used to measure the equilibrium surface pressures of spread monolayers using monolayer deposition methods, as described previously.<sup>6,8,9</sup> A specific amount of phospholipid dissolved in organic solvent was deposited on a surface of known area per molecule ( $A_m$ ). Depending on the monolayer state, 1 to 24 h after the solvent evaporated was required for the monolayer to attain an apparent equilibrium. The equilibrated monolayer-to-bilayer collapse surface pressure and the molecular area at collapse are expressed as  $\pi_c$  and  $A_c$ , respectively.

**(d) Surface Fluorescence Microscopy of Phospholipid Monolayers.** Monolayer phase behavior was directly visualized by fluorescence microscopy (FM).<sup>26–30</sup> The fluorescence microscope was constructed in this laboratory, as described previously.<sup>6–8</sup> The phospholipid fluorophore, NBD-PC (Avanti Polar Lipids, Alabaster, AL), concentration (1 mol %), subphase temperature, air temperature, relative humidity, and data acquisition were identical to the conditions used earlier.<sup>6,9</sup>

**(e) Water Vapor Sorption and Desorption Using a Gravimetric Sorption Analyzer.** Water vapor sorption isotherms were measured gravimetrically at 25 °C using an automated microelectronic balance coupled to a computerized Model MB 300G VTI sorption analyzer (VTI Corp., Hialeah, FL) under vacuum conditions, as described earlier.<sup>25</sup> A sample of approximately 3.00–5.00 mg was loaded onto the hanging aluminum sample pan and the glass jackets of both the hanging sample and reference pans were closed and

clamped securely. The criterion used to establish absorption/desorption equilibrium was a weight change of less than or equal to 0.03% in a 7–10-min interval. Each isotherm reported represents the average of at least two complete cycles on different samples.

**(f) Hot-Stage Optical Light Microscopy.** “Dry” samples were visually examined using hot-stage optical light microscopy under cross polarizers with an Olympus BH-2 optical microscope with a sample heating/cooling stage (THMS 600 heating/freezing stage) and a temperature programmer (TMS 92 Linkam, Scientific Instrument Ltd., Waterfield, Tadworth, Surrey, KT20 5HT, England). A heating rate of 5.0 °C/min was used.

**(g) Circular Dichroism and Surface Dichroism Spectroscopy.** Circular dichroism (CD) measurements for both bulk and monolayer systems at the air/water interface *in situ* were performed on an OLIS (On Line Instrument Systems, Inc., Jefferson, GA) 4100C Spectrophotometer at room temperature with the light beam oriented in the vertical mode, unlike conventional circular dichroism spectrometers where the light passes through horizontally. The computerized modified instrument, previously reported,<sup>22</sup> contains a double beam CD spectrometer that is created by splitting the light beam before it passes through the CD modulator in order to enhance the signal-to-noise ratio. One of the beams passes through a reference PM detector, while the other beam passes through the CD modulator, the Langmuir trough, and then finally to the photomultiplier (PM) detector. A specially designed aluminum with black Teflon coated Langmuir trough (18.5 cm × 5.5 cm × 1.1 cm) with a 2.5 cm diameter quartz (Suprasil quartz) window at the bottom of the trough was used for surface circular dichroism measurements.<sup>22</sup> The sample compartment chamber was then sealed to prevent evaporation of the liquid in the trough and to prevent any outside light from coming in and causing interference. The wavelength scanning range was 190 nm –240 nm (far UV or peptide region of the spectrum) in 0.5 nm increments using a Xenon lamp as the light source that was cooled throughout the experiments with a continuous flow of in-house chilled water. To prevent the sample accumulation of oxygen, which produces CD absorption bands around 200nm, during experiments, a steady flow of a nitrogen gas purge was present. The liquid height in the trough was 1 cm, and the bandwidth was 1 nm. Each scan over the stated scanning range took 3 min, and 30 consecutive scans were acquired for an average scan CD curve at a given surface pressure. Sampling frequency was 28 per second at 0.5 nm wavelength increments. Average of 30 scans for pure water at room temperature were taken as the baseline and subtracted from final average monolayer CD scans. After the baseline scan for water was acquired, the surface was suctioned off with a Pasteur pipet and the monolayer was deposited at a given area/molecule. After the solvent evaporated and equilibrium was attained, which took 1–12 h depending on the surface concentration, 30 scans were taken and averaged. The CD data were recorded as ellipticity in millidegrees.

- (26) Knobler, C. M. Seeing Phenomena in Flatland: Studies of Monolayers by Fluorescence Microscopy. *Science* **1990**, *249*, 870–874.
- (27) Stine, K. J.; Knobler, C. M. Fluorescence Microscopy: A Tool for Studying the Physical Chemistry of Interfaces. *Ultramicroscopy* **1992**, *47*, 23–34.
- (28) McConnell, H. M.; Tamm, L. K.; Weis, R. M. Periodic Structures in Lipid Monolayer Phase Transitions. *Proc. Natl. Acad. Sci. U.S.A.* **1984**, *81*, 3249–3253.
- (29) McConnell, H. M. Structures and Transitions in Lipid Monolayers at the Air-Water Interface. *Annu. Rev. Phys. Chem.* **1991**, *42*, 171–195.
- (30) Nag, K.; Boland, C.; Rich, N. H.; Keough, K. M. W. Design and Construction of an Epifluorescence Microscopic Surface Balance for the Study of Lipid Monolayer Phase Transitions. *Rev. Sci. Instrum.* **1990**, *61*, 3425–3430.

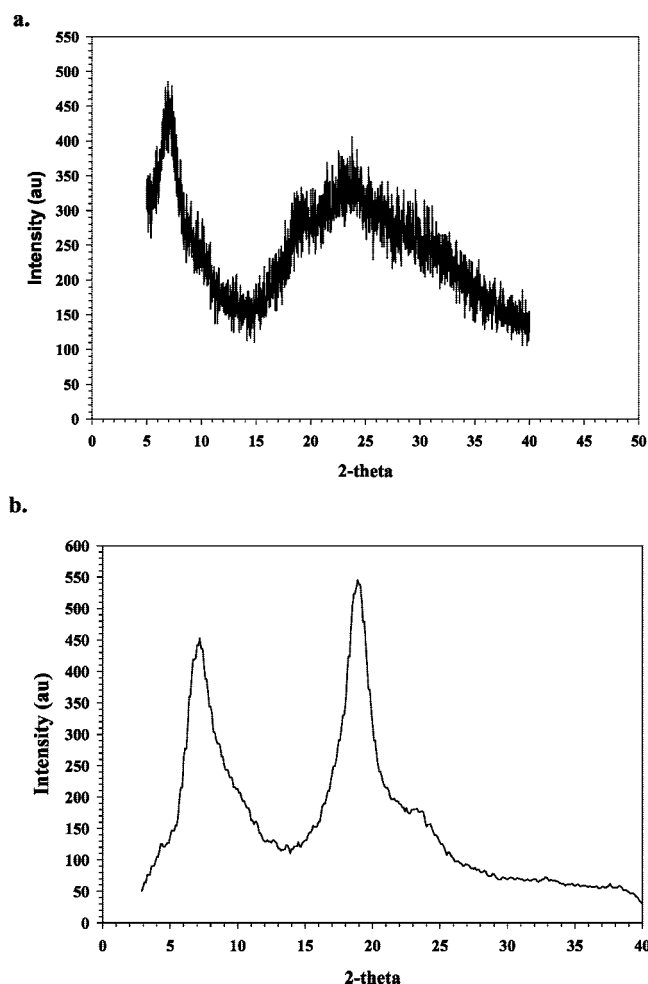


**Figure 1.** X-ray powder diffractograms (a. slit-detector; b. area-detector) of KL<sub>4</sub> powder at 25 °C

**(h) X-Ray Powder Diffraction (XRPD).** Two different types of X-ray diffraction instruments were used; an area detector and a slit detector. One X-ray diffraction unit used (area detector) was a Siemens General Area Detector Diffraction System (Siemens, Madison, WI). The X-rays were generated with a Cu K $\alpha$  source (40kV, 20mA). Glass capillaries of 2 mm i.d. (Charles Supper Co., Natick, MA) held the sample and were placed in the X-ray beam path, and rotated 360° within the beam during the diffraction data collection over the scanning range of 3 to 40 two-theta degrees at room temperature. The other X-Ray Diffraction instrument (slit detector) was a Scintag PADV X-ray Diffractometer (Scintag Inc., Santa Clara, CA) with a Cu K $\alpha$  source at 40 mA and 30 kV. The scanning range of 5 to 40 two-theta degrees at room temperature was used at a scanning rate of 2.5 two-theta degrees per minute at a step rate of 0.02 two-theta degrees.

## Results

**Properties of KL<sub>4</sub>. (a) Secondary Structural Properties of KL<sub>4</sub> in the Solid-State.** Shown in Figure 1 are two powder X-ray diffractograms (Figure 1a is from a slit detector and Figure 1b is from an area detector) at 25 °C showing peaks at 7 2θ and 19 2θ with a shoulder at 23.5 2θ. It appears

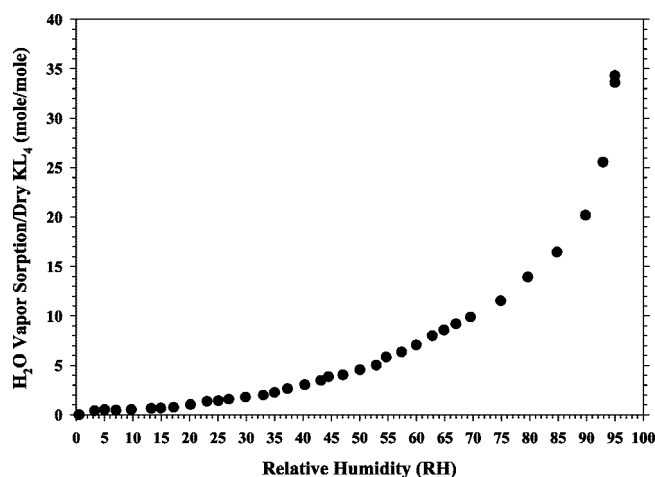


**Figure 2.** Water vapor sorption isotherm of KL<sub>4</sub> at 25 °C, following preconditioning at 25 °C (●).

from the spectra that KL<sub>4</sub> in the “dry” state exhibits defined structure, similar to that observed in small molecule liquid crystals and certain heteropolypeptides having  $\alpha$ -helical and  $\beta$ -sheet secondary structure conformations.<sup>31</sup> Thermal analysis of dry KL<sub>4</sub> powder using DSC at a scanning rate of 1.0 °C/minute (thermogram not shown), indicates that no detectable enthalpic phase transitions occur during the first and second heating scans over a wide temperature range. Hot-stage microscopy (images not shown) of KL<sub>4</sub> powder from 25 to 75 °C showed birefringence under cross-polarizers. This seems to indicate that KL<sub>4</sub> in the solid state has a significant degree of order, perhaps due to some kind of secondary structure or liquid crystalline nature.

**(b) Water Vapor Sorption Behavior of KL<sub>4</sub> in the Solid-State.** Given the hydrophilic properties of KL<sub>4</sub> due to the lysine residues (−0.99 lysine hydrophobic parameter),<sup>32</sup> and its hydrophobicity due to the leucine residues (1.70 leucine hydrophobic parameter),<sup>32</sup> it was of interest to examine the water vapor sorption tendencies of KL<sub>4</sub>. Figure 2 shows that the water vapor sorption profile is typical of a “BET-Type III” isotherm with a continually significant increase in water uptake as the relative humidity (RH) increases but relatively low at lower relative humidities. For example, at 95%RH, as much as 35 moles of water per mole of KL<sub>4</sub> were absorbed; whereas at 20%RH, about 1 mol of water per mole of KL<sub>4</sub> was absorbed. The water vapor sorption and desorption behavior for phospholipids in the solid-state, in general, and for DPPC and POPG in particular, is significantly different, as reported in a detailed study by Mansour and Zografi.<sup>25</sup>

**(c) Surface Properties of KL<sub>4</sub>.** The equilibrium spreading pressure,  $\pi_e$ , of KL<sub>4</sub> at 25 °C has a value of  $32.6 \pm 0.3$  mN/m, in agreement with earlier studies,<sup>10</sup> and, essentially,

(31) Katakai, R.; Iizuka, Y. Conformation of Oligopeptides with L-Leucyl-L-Leucyl-L-Alanyl and L-Methionyl-L-Methionyl-L-Leucyl Repeating Units. *Biopolymers* **1984**, 23, 1411–1422.

(32) Fauchere, J.; Pliska, V. Hydrophobic parameters  $\pi$  of amino acid side chains from the partitioning of N-acetyl-amino-acid amides. *Eur. J. Med. Chem.* **1983**, 18, 369–375.

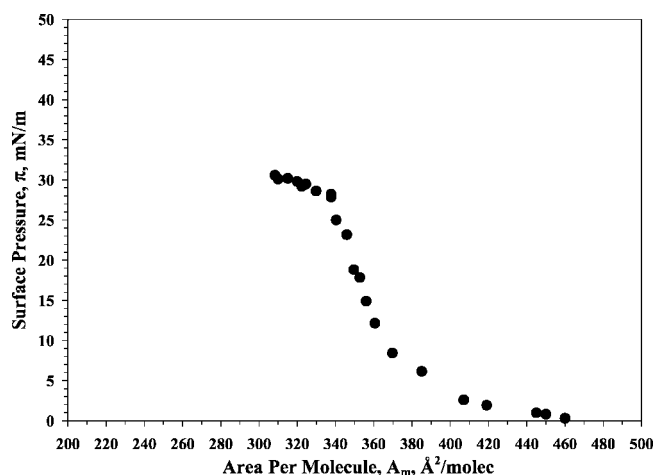


**Figure 3.** Surface pressure ( $\pi$ ) vs area per molecule ( $A_m$ ) isotherm at 25 °C for KL<sub>4</sub> monolayers at the air–water interface, spread on pH 7.4 Tris buffer with 150 mM NaCl.

remains constant (time-independent) at an equilibrated value of  $32.8 \pm 0.1$  mN/m as the temperature is increased to 37 °C. The spreading was observed to be instantaneous within seconds and remained stable for at least twenty-four hours, indicating the KL<sub>4</sub> forms a stable insoluble film at an air–water interface.

The surface pressure–area ( $\pi$ – $A$ ) isotherm of KL<sub>4</sub> at 25 °C, as shown in Figure 3, further indicates that KL<sub>4</sub> on pH 7.4 150 mM NaCl buffer subphase forms a stable insoluble monolayer at the air–water interface. This  $\pi$ – $A$  isotherm is significantly shifted to the right (higher  $A_m$  at a given  $\pi$ ) of the KL<sub>4</sub> equilibrium monolayer isotherms determined earlier at 25 °C;<sup>10</sup> this may be due to the difference in purity of the two samples (>99% vs 87%) and/or the presence of different subphase counterion (acetate in the earlier studies vs chloride in this study). The monolayer appears to be highly expanded (as noted by the high area per molecule,  $A_m$ ) with no detectable surface phase transition, except at monolayer collapse; this was found to occur at  $\pi_c$  about 30 mN/m, in good agreement with  $\pi_e$ . Single-shot monolayer studies at 37 °C also indicated that  $\pi_c$  occurs around 30 mN/m.

**(d) Secondary Structure of KL<sub>4</sub> in Solution.** Assuming that conformational structure may play an important role in the surface properties of KL<sub>4</sub> at an air–water interface, given the presence of cationic and hydrophobic residues, it was of interest to investigate the structural properties of KL<sub>4</sub> in bulk solution (three-dimensional state), and later, at the air–water interface (two-dimensional state). As would be expected and is generally accepted, the chloroform:methanol cosolvent produces a “noisy” baseline CD spectrum (not shown) that interferes with the CD spectra of peptides and proteins. Figure 4 shows the solution CD spectrum of KL<sub>4</sub> in acetonitrile:water 40:60 cosolvent systems carried out at room temperature. The solution CD spectra for KL<sub>4</sub> in the acetonitrile:water cosolvent system (produces a good baseline) indicate that KL<sub>4</sub> exhibits  $\alpha$ -helical secondary structure, in excellent agreement with previous unpublished reports (private communications, N. Williams, R. W. Johnson

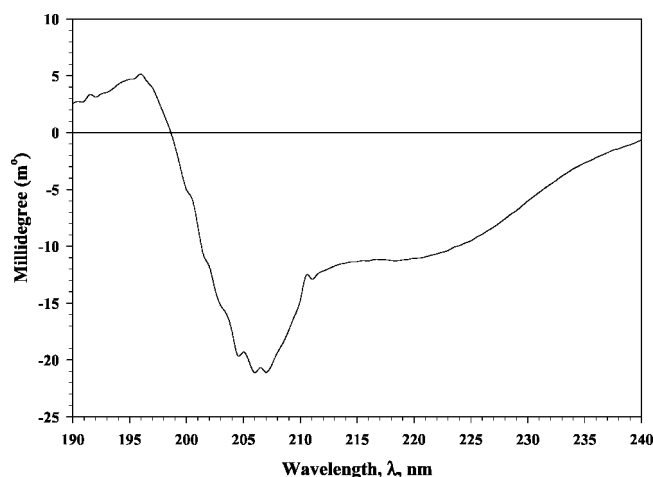


**Figure 4.** Solution circular dichroism ( $m^\circ$ ) of KL<sub>4</sub> in acetonitrile:H<sub>2</sub>O cosolvent at 25 °C (—).

Pharmaceutical Research Institute) and with published solution CD of solution conformation (i.e., three-dimensional conformation) KL<sub>4</sub> in different organic solvents and lipid environments.<sup>14,33,34</sup>

**(e) Secondary Structure of KL<sub>4</sub> in the Monolayer State at the Air–Water Interface.** In initial studies using the Tris NaCl buffer system, an intense CD signal due to the chloride ion is observed just below 200 nm (CD spectrum not shown), which is also where some protein/peptide secondary structural CD peaks can also be observed. This was expected to occur, since the chloride ion is well-known to mask solution protein/peptide CD signals at 200 nm and below. Therefore, for all subsequent surface CD studies, the subphase used was triply distilled water at room temperature under a gentle nitrogen gas stream (as described in the Experimental Methods). Indeed, the CD spectrum (Figure 5a) of pure water does not show any significant peaks in the 240–190 nm range. The small peaks between 195 nm and 190 nm are believed to be reflective of the hydrogen-bonding nature of water. Figure 5b shows the baseline-corrected CD spectrum of the KL<sub>4</sub> monolayer equilibrated at a surface pressure of 5 mN/m. The peaks found in the CD spectrum of equilibrated KL<sub>4</sub> monolayer indicate that, even at such a low surface pressure, KL<sub>4</sub> appears to assume a well-defined secondary conformation at the air–water interface. The magnitude of the CD signal of KL<sub>4</sub> monolayers at 15 mN/m is significantly intensified, as shown in Figure 5c, more clearly indicating the presence of a secondary conformation of KL<sub>4</sub> at the surface. When the surface pressure of KL<sub>4</sub> is increased to 25 mN/m (Figure 6), the CD signal is similar in intensity to that observed at 15 mN/m, suggesting that

- (33) Nilsson, G.; Gustafsson, M.; Vandenbussche, G.; Veldhuizen, E.; Girffiths, W. J.; Sjoval, J.; et al. Synthetic peptide-containing surfactants: evaluation of transmembrane versus amphipathic helices and surfactant protein C poly-valyl to poly-leucyl substitution. *Eur. J. Biochem.* **1998**, 255, 116–124.
- (34) Saenz, A.; Canadas, O.; Bagatolli, L. A.; Johnson, M. E.; Casals, C. Physical properties and surface activity of surfactant-like membranes containing the cationic and hydrophobic peptide KL<sub>4</sub>. *FEBS J.* **2006**, 273, 2515–2527.

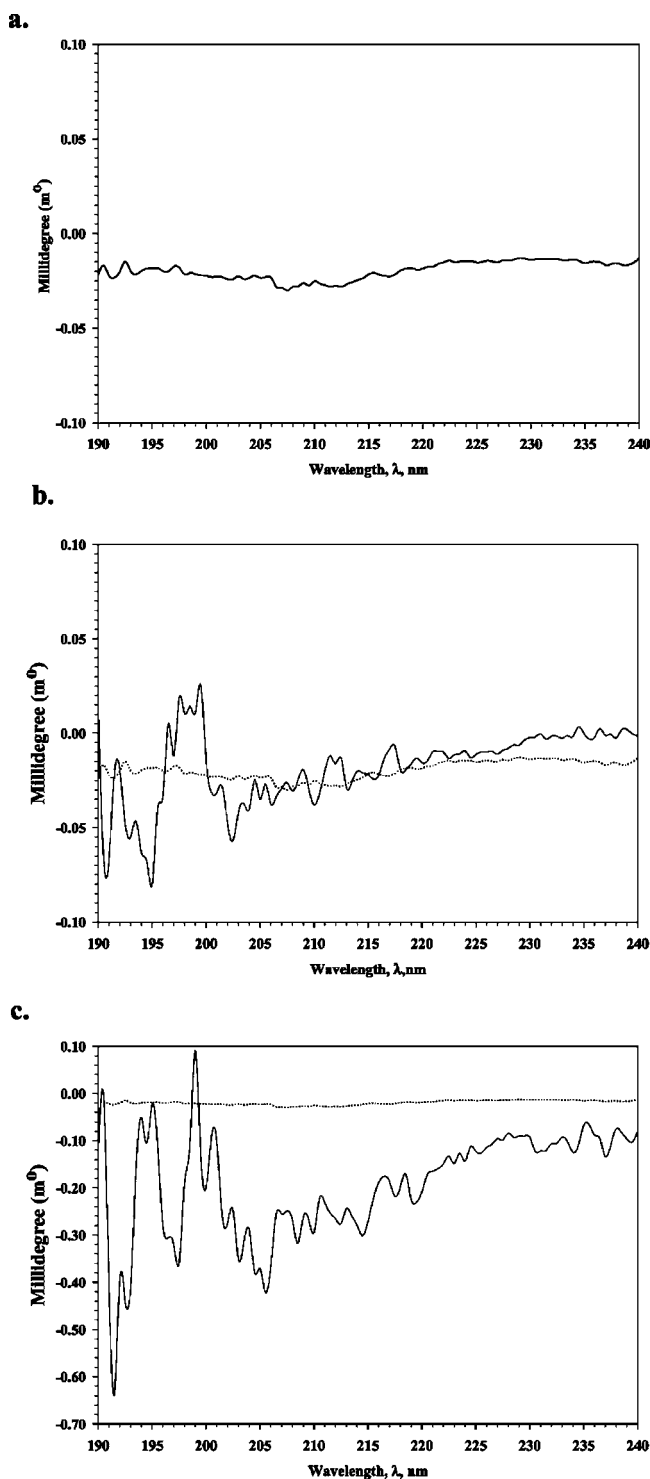


**Figure 5.** Surface circular dichroism (m°) of triply distilled water at 25 °C of (a) water (—); (b) water (···) and monolayer KL<sub>4</sub> equilibrated at  $\pi = 5$  mN/m at the air–water interface (—); (c) water (···) and monolayer KL<sub>4</sub> equilibrated at  $\pi = 15$  mN/m at the air–water interface (—).

the conformation of KL<sub>4</sub> in these surface pressure regions of the monolayer isotherm is the same. Furthermore, this also suggests that the two-dimensional rotational motion in the plane of the monolayer is similar.

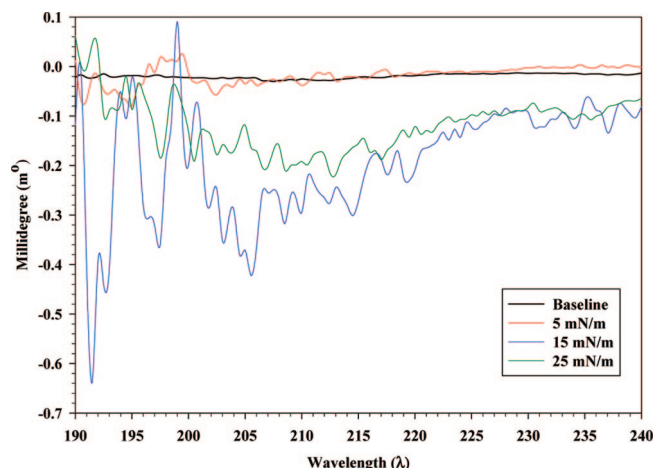


**Figure 6.** A comparison of the surface circular dichroism (m°) of KL<sub>4</sub> monolayers at various surface pressures ( $\pi$ ) spread on triply distilled water at 25 °C.

#### Properties of Mixtures of Phospholipids and KL<sub>4</sub>.

**(a) Bilayer Mixtures of Phospholipids and KL<sub>4</sub>.** Given that the thermal analysis of dry KL<sub>4</sub> indicated a lack of any detectable thermal events (as presented earlier in the Results), it was not surprising to find that the presence of KL<sub>4</sub> in DPPC/KL<sub>4</sub> and POPG/KL<sub>4</sub> mixtures did not appear to change the gel-to-liquid crystalline main phase transition temperature,  $T_m$ , of fully hydrated colloidal dispersions of DPPC and POPG bilayers. These  $T_m$  values were similar to the  $T_m$  values of the single-component fully hydrated phospholipids reported earlier by Mansour and Zografi.<sup>6,25</sup> Therefore, it was of interest to see if KL<sub>4</sub> affected the equilibrium spreading pressures,  $\pi_e$ , of DPPC and POPG bilayers. Shown in Table 1 are the rounded values of  $\pi_e$  at 25 °C, 37 °C, and 45 °C for various compositions of DPPC/KL<sub>4</sub>, POPG/KL<sub>4</sub>, and DPPC/POPG/KL<sub>4</sub> mixtures at the air–water interface. It can be seen that, at 25 and 37 °C,  $\pi_e$  is about 32 mN/m for the various DPPC/KL<sub>4</sub> compositions, whereas the  $\pi_e$  of gel DPPC alone ( $T_m = 41$  °C)<sup>6</sup> is about 0.2 mN/m and KL<sub>4</sub> alone is 32 mN/m. This is in contrast to  $\pi_e$  of 45 mN/m for DPPC/KL<sub>4</sub> mixtures at 45 °C (above the  $T_m$  of DPPC), which is identical to the spreading of liquid crystalline DPPC alone at this temperature.<sup>6</sup> For POPG/KL<sub>4</sub> dispersions, at all three temperatures, spreading to a value of ~46 mN/m occurred, which is identical to the spreading of liquid crystalline POPG alone at these temperatures.<sup>6</sup> For the ternary system, DPPC/POPG/KL<sub>4</sub> 75:24:1, it can be seen that maximal spreading to an equilibrium value ~45 mN/m occurred at all three temperatures. As recently reported,<sup>9</sup> DPPC/POPG fully hydrated bilayer systems exhibit monotectic phase behavior and phase separation of the individual components in the two-gel state region. Thus, DPPC/POPG 75:25 has an intermediate bilayer main phase transition temperature and a  $\pi_e$  value of <0.2 mN/m at 25 °C, which is indicative of the formation of a gaseous monolayer.<sup>6,9</sup> Thus, the presence of a small amount of KL<sub>4</sub> cationic hydrophobic heteropolymer promotes the spreading of the DPPC/POPG 75:25 phospholipid mixtures, in agreement with earlier observations.<sup>10</sup>



**Table 1.** The Equilibrium Spreading Pressures (Rounded Values),  $\pi_e$ , of Mixtures of the Cationic Hydrophobic Heteropolypeptide, KL<sub>4</sub>, and Phospholipid Bilayers, at the Air–Water Interface at 25°C, 37°C, and 45°C

binary mixture	equilibrium spreading pressure $\pi_e$ (mN/m)		
	25 °C	37 °C	45 °C
DPPC/KL <sub>4</sub>			
100:0	≤0.2	≤0.2	45
99:1	32	32	45
96:4	32	32	45
93:7	32	32	45
90:10	32	32	45
0:100	32	32	32
POPG/KL <sub>4</sub>			
100:0	46	46	46
99:1	46	46	46
96:4	46	46	46
93:7	46	46	46
90:0	46	46	46
0:100	32	32	32
DPPC/POPG/KL <sub>4</sub>			
75:24:1	44	45	45
75:25:0	≤0.2	46	46

**(b) Monolayer Mixtures of Phospholipids and KL<sub>4</sub>.** Figure 7 shows the  $\pi$ – $A$  isotherms at 25 °C for monolayers at the air–water interface for DPPC/KL<sub>4</sub> 96:4 (Figure 7a), POPG/KL<sub>4</sub> 96:4 (Figure 7b), and DPPC/POPG/KL<sub>4</sub> 75:25:1 (Figure 7c), all of which are shifted to higher areas per molecule at a given surface pressure (compared with phospholipid alone) due to the presence of KL<sub>4</sub> in the monolayer (see Figure 3). The DPPC/KL<sub>4</sub> binary mixtures (Figure 7a) exhibit a distinct LE/LC surface phase transitions (verified with surface fluorescence microscopy) at an invariant liquid-expanded (LE)-to-liquid condensed (LC) surface phase transition pressure,  $\pi_t$ , at a value that is nearly identical to that of  $\pi_t$  of DPPC monolayers alone under time-independent equilibrium conditions.<sup>6,8</sup> The value of the monolayer equilibrium collapse surface pressure,  $\pi_c$ , is similar to the value of  $\pi_c$  for equilibrated DPPC monolayers,<sup>6</sup> namely, a  $\pi_c$  value of ~45 mN/m. The area at collapse, defined as  $A_c$ , for DPPC<sup>6</sup> and DPPC/KL<sub>4</sub> monolayers appear to be very similar ( $\pm 0.3$  Å<sup>2</sup>/molecule), as well. Under equilibrium, time-independent conditions, the presence of KL<sub>4</sub> appears to have little impact on the nature of the DPPC monolayer, i.e.  $\pi_t$ ,  $A_c$ , and  $\pi_c$ .

This is in contrast to equilibrated POPG/KL<sub>4</sub> monolayer mixtures under time-independent conditions, as shown Figure 7b. At high areas per molecule ( $A_m$ ), the liquid expanded (LE) regions of both the POPG<sup>6</sup> and POPG/KL<sub>4</sub> time-independent equilibrated monolayer isotherms appear to be nearly identical, as are the  $\pi_c$  values (~45 mN/m). However, near 15 mN/m and higher, the isotherms become significantly different. The POPG/KL<sub>4</sub> monolayer mixtures appear to have a steeper slope than that of POPG alone. Furthermore, the areas at collapse ( $A_c$ ) are significantly different, where the

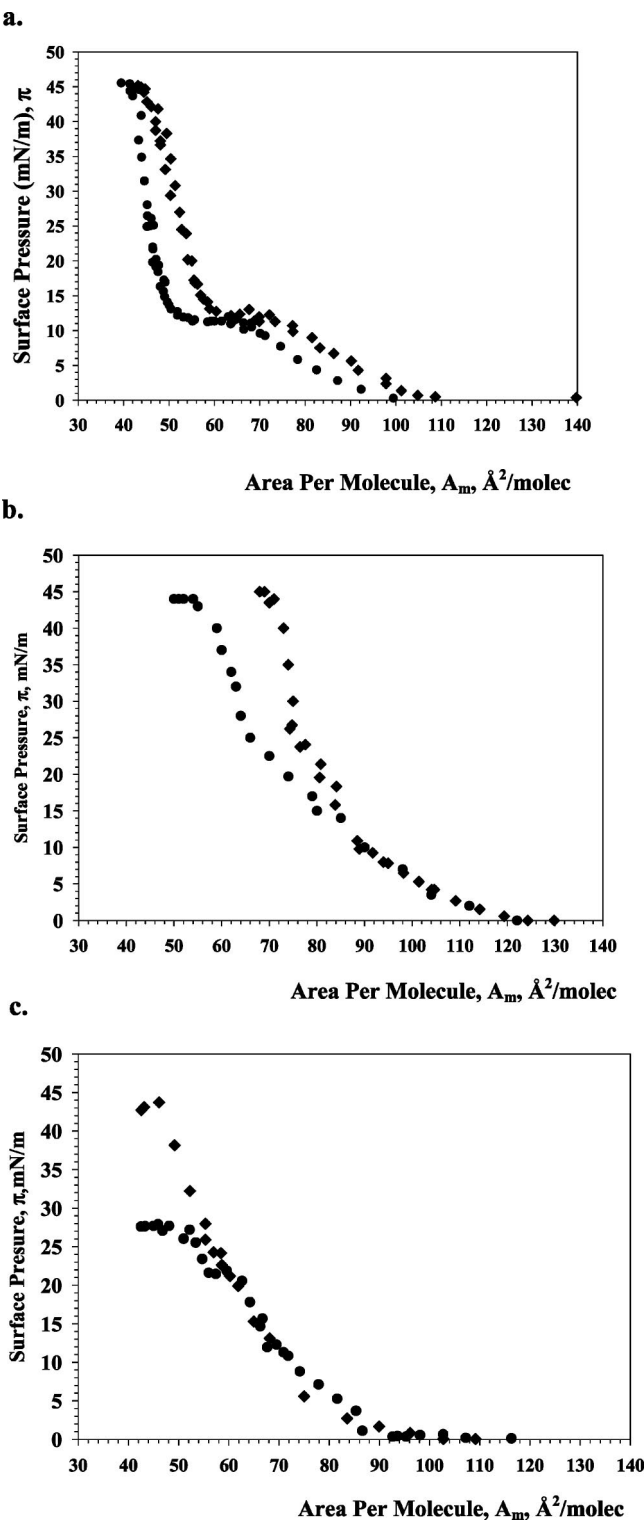


**Figure 7.** Surface pressure ( $\pi$ ) vs area per molecule ( $A_m$ ) isotherms for monolayers at the air–water interface spread on pH 7.40 TRIS buffer with 150 mM NaCl at 25 °C for (a) DPPC (●) and DPPC/KL<sub>4</sub> 96:4 (◆); (b) POPG (●) and POPG/KL<sub>4</sub> 96:4 (◆); and (c) DPPC/POPG 75:25 (●) and DPPC/POPG/KL<sub>4</sub> 75:24:1 (◆).

$A_c$  ( $\pm 0.3$  Å<sup>2</sup>/molecule) of the binary mixture is significantly higher than that of POPG.<sup>6</sup>



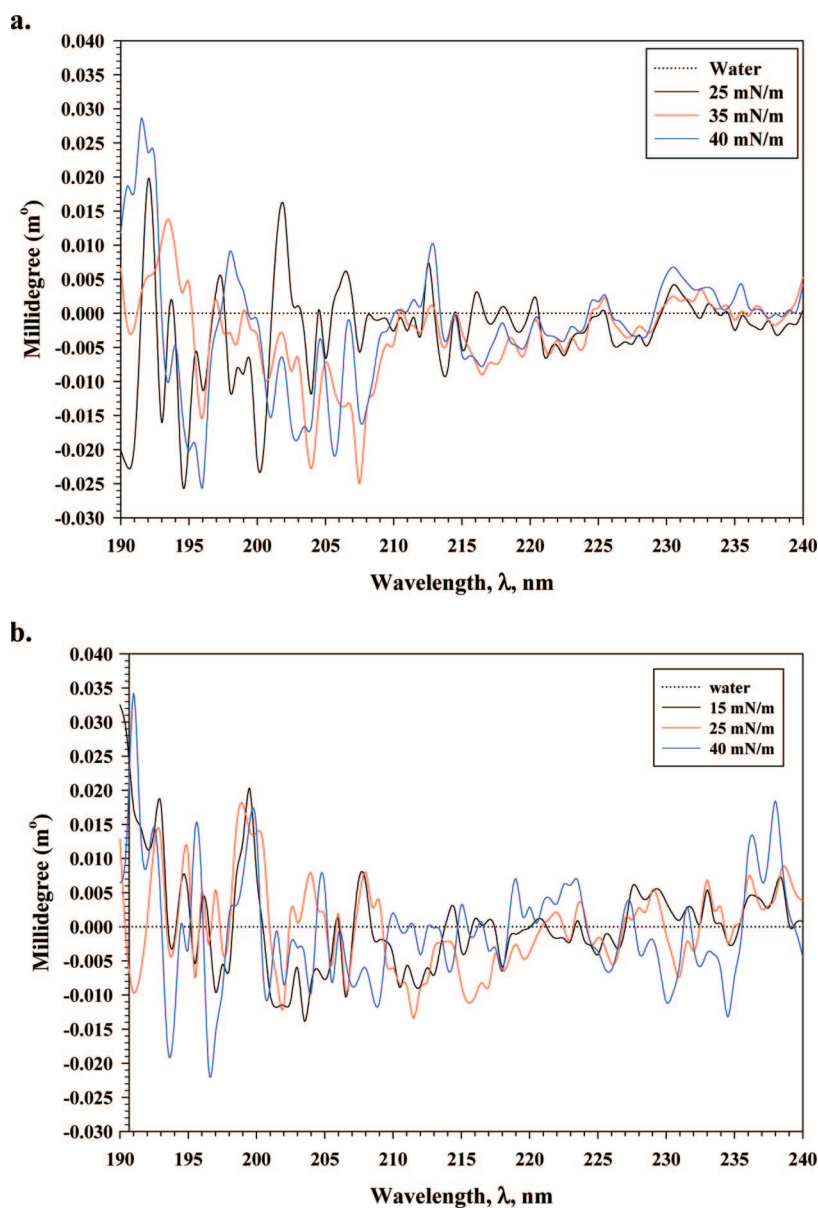


**Figure 8.** The surface circular dichroism ( $m^\circ$ ) of phospholipid/KL<sub>4</sub> 50:50 monolayers at various surface pressures at 25 °C: (a) DPPC/KL<sub>4</sub>; and (b) POPG/KL<sub>4</sub>.

The presence of KL<sub>4</sub> in a DPPC/POPG 75:25 monolayer has a very significant effect on equilibrium monolayer collapse, as shown in the time-independent monolayer isotherms (Figure 7c). DPPC/POPG 75:25 monolayer molar composition corresponds to the bilayer molar composition that falls in the equilibrium gel–liquid crystalline coexistence region of the equilibrium bilayer thermotropic phase diagram.<sup>9</sup> Additionally, under equilibrium conditions, the DPPC/POPG 75:25 monolayer collapses to form and coexist with its self-assembled bulk phase (bilayers) at a collapse surface pressure value ( $\pi_c$ ) of 28 mN/m. This  $\pi_c$  value (28 mN/m) for a DPPC/POPG 75:25 monolayer is significantly lower than the maximum time-independent  $\pi_c$  value of the individual DPPC and POPG equilibrated monolayers at 25 °C, where a maximum time-independent  $\pi_c$  value of  $\sim 45$  mN/m is attained at equilibrium.<sup>6,9</sup> Also, under equilibrium conditions, DPPC and POPG phospholipid molecules are miscible

with one another in both the bilayer and monolayer states, as reflected in the bilayer thermotropic phase diagram and in the equilibrium monolayer surface phase diagram.<sup>9</sup> Consequently, the miscibility of DPPC and POPG is accompanied with the reduction in the time-independent equilibrium values of  $\pi_c$  and  $\pi_e$  from their maximum time-independent value of 45 mN/m to a time-independent intermediate value of  $\sim 28$  mN/m.<sup>9</sup> However, once KL<sub>4</sub> is introduced into these equilibrated DPPC/POPG binary mixture systems, a time-independent  $\pi_c$  value of 45 mN/m is attained under equilibrium conditions, in good agreement with earlier reports.<sup>10</sup>

**(c) Secondary Structure of KL<sub>4</sub> in Phospholipid Monolayers at the Air–Water Interface.** Figure 8 shows the surface CD spectra at DPPC/KL<sub>4</sub> 50:50 and POPG/KL<sub>4</sub> 50:50 monolayers at 25 °C on water, respectively. The spectra clearly indicate the presence of KL<sub>4</sub> secondary

structures. As it would be expected in phospholipid systems, DPPC and POPG monolayers, in the absence of KL<sub>4</sub>, were observed to have no secondary structure, as indicated by the lack of a CD signal using surface CD (CD spectra not shown).

## Discussion

The purpose of this reported study was to synthesize KL<sub>4</sub> in a very high state of purity (>99%), to characterize the equilibrium thermal, structural, and surface properties of KL<sub>4</sub> alone (as a solid, solution, and at an air–water interface using *in situ* surface CD) and in the presence of DPPC and POPG phospholipids, and to explore its effect on DPPC and POPG spreading on a pH 7.4 Tris NaCl buffer system at 25 and 37 °C at various molar compositions in both the bilayer and monolayer states.

One of the important observations in this study is that KL<sub>4</sub> cationic hydrophobic heteropolypeptide spreads from the bulk state (three-dimensional) and forms a stable insoluble monolayer (two-dimensional state) at the air–water interface, confirming earlier results.<sup>10</sup> Analyzing the KL<sub>4</sub> isotherm at 25 °C reveals that lift-off (defined as the area per molecule where intermolecular interactions between adjacent surface-active component molecules in the monolayer begin to be “felt”) occurs at an  $A_m$  value of approximately 450 Å<sup>2</sup>/KL<sub>4</sub> molecule. Given that KL<sub>4</sub> is a 21-amino acid heteropolypeptide, this gives approximately 21 Å<sup>2</sup>/amino acid, which is in excellent agreement with the biochemical literature result of approximately 20 Å<sup>2</sup>/amino acid for amphiphilic proteins on the surface, in general, and for SP-B,<sup>35</sup> in particular.

Another important observation made in this study, confirming earlier results<sup>10</sup> under different conditions, is that KL<sub>4</sub> has a significant effect on the surface properties of both DPPC/POPG 75:25 and POPG bilayers (various compositions) and monolayers (96:4 and 90:10), but not on DPPC bilayers (various compositions) and monolayers (96:4 and 90:10). In the study of miscibility in monolayers, binary mixtures can be treated as two-dimensional solutions.<sup>36</sup> For binary mixtures exhibiting ideal mixing or complete immiscibility, average molecular area,  $A_{av}$ , can be shown to be related to that of the individual components as

$$A_{av} = N_1 A_1 + N_2 A_2 \quad (1)$$

where  $A_1$  and  $A_2$  are the area per molecule of each monolayer component at constant surface pressure, and  $N_1$  and  $N_2$  are their respective mole fractions. Nonideal miscible monolayers arise because of interactions between the components that lead to deviations from the additivity rule reflected in the parameter  $A^E$ , the excess area.  $A^E$  is defined as

$$A^E = A_{12} - A_{av} \quad (2)$$

Therefore,

$$A^E = A_{12} - (N_1 A_1 + N_2 A_2) \quad (3)$$

where  $A_{12}$  is the experimentally measured area per molecule of the mixed monolayer and  $A_{av}$  is the calculated molar-weighted average isotherm (ideal monolayer isotherm).

Nonideal miscible monolayers arise from interactions between the components leading to deviations from the additivity rule through the parameter  $A^E$ , the excess area. When  $A^E = 0$ , either ideal mixing or complete immiscibility occurs. When  $A^E > 0$ , miscibility occurs and positive deviations from the predicted area occur due to greater interactions between the individual monolayer components with themselves (A–A interactions) than between the two different components (A–B interactions). When  $A^E < 0$ , miscibility occurs and negative deviations from the predicted area occur as a result of greater attractive A–B interactions between the different monolayer components. Specifically, as shown in Figure 9, two-dimensional excess area analysis indicates that  $A^E = 0$  for DPPC/KL<sub>4</sub> monolayers at the studied compositions of 96:4 (shown) and 90:10 (not shown). The ideal mixing is also reflected in the similar values of  $A_c$  and other aspects of the monolayer isotherms of the DPPC/KL<sub>4</sub> mixture and DPPC alone. Given that  $A^E = 0$  is ideal mixing, this can mean either complete ideal miscibility or complete immiscibility. From the spreading data, it becomes clear that DPPC and KL<sub>4</sub> are indeed completely phase separated in the bilayer and monolayer states. In addition, thermal analysis reveals that no significant change in  $T_m$  of fully hydrated DPPC bilayers occurs at in the presence of KL<sub>4</sub> (at the compositions studied). The mixing of POPG and KL<sub>4</sub> reveals that nonideal mixing ( $A^E \neq 0$  Å<sup>2</sup>/molecule) occurs such that POPG/KL<sub>4</sub> 96:4 (shown) and 90:10 (not shown) mixtures exhibit monolayer condensation at lower areas per molecule (steep slope approaching monolayer collapse), and the value of  $A_c$  is significantly larger for the mixture than for that for POPG alone. For this binary mixture system,  $A^E$  is less than zero ( $A^E < 0$  Å<sup>2</sup>/molecule), indicating that there is net attractive interaction between POPG and KL<sub>4</sub> molecules. Near 10 mN/m surface pressure for POPG/KL<sub>4</sub> monolayer, a minimum  $A^E$  value (–12 Å<sup>2</sup>/molecule) is observed indicative of maximum deviation from ideality and significant condensation of the binary mixture monolayer. At surface pressures below and above 10 mN/m,  $A^E$  values remain significantly <0 Å<sup>2</sup>/molecule but greater than –12 Å<sup>2</sup>/molecule. This seems to suggest that KL<sub>4</sub> condenses POPG in the monolayer state at all equilibrium surface pressures. Furthermore, at a surface pressure around 23 mN/m, it appears that a LE/LC surface phase transition occurs over a very narrow  $A_m$  range. Spreading data also indicates that spreading from the three-dimensional bulk state to the two-dimensional state (monolayer) spontaneously occurs resulting in a time-independent  $\pi_c$  value of 46 mN/m. This  $\pi_c$  value is equal to the time-independent equilibrium value of monolayer  $\pi_c$ , where the three-dimensional state self-assembles and coexists at equilibrium with its monolayer state.

Favorable electrostatic interactions can occur between cationic hydrophobic KL<sub>4</sub> and anionic POPG, as has been

(35) Taneva, S.; Keough, K. Pulmonary Surfactant Proteins SP-B and SP-C in Spread Monolayers at the Air–Water Interface: I. Monolayers of Pulmonary Surfactant Protein SP-B and Phospholipids. *Biophys. J.* **1994**, *66*, 1137–1148.

(36) Gaines G. *Insoluble Monolayers at the Liquid–Gas Interfaces*; Interscience Publishers: New York, 1966.

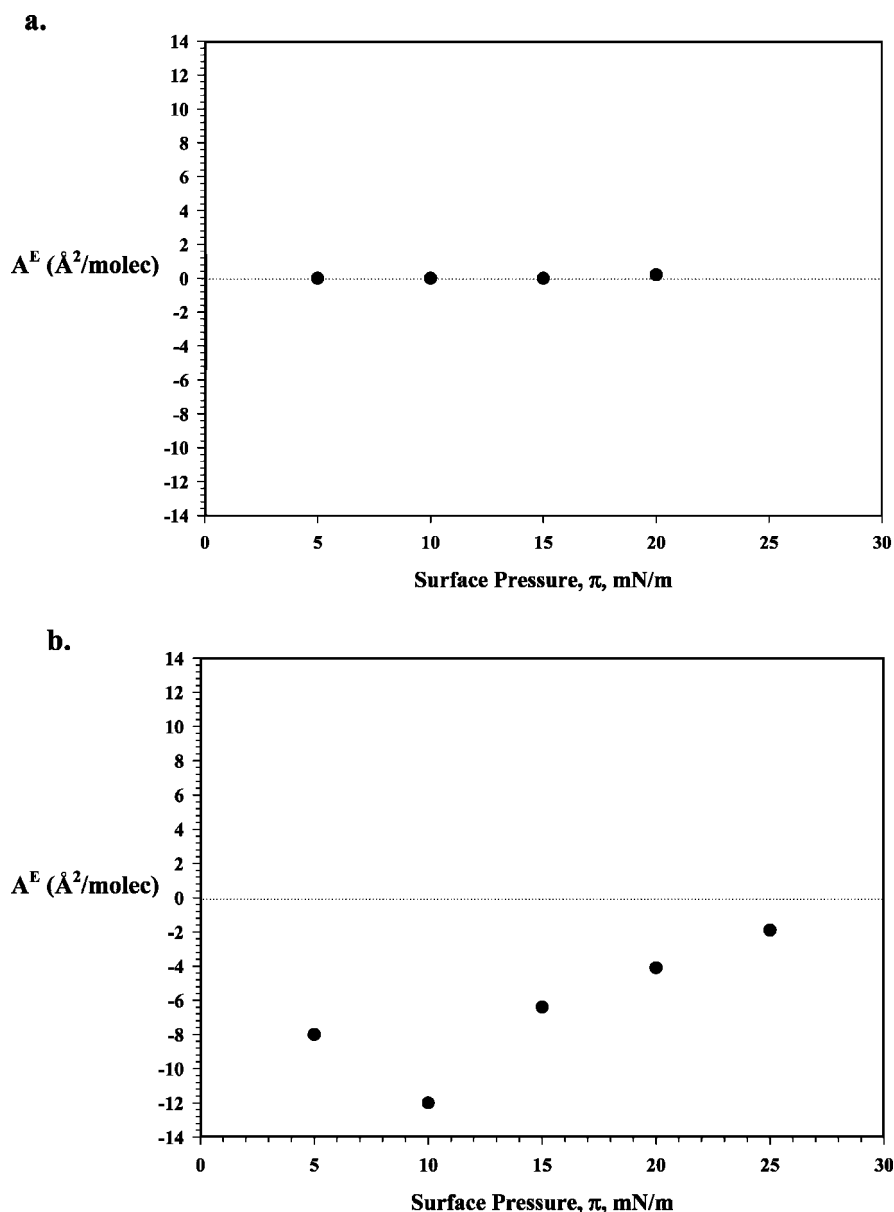


**Figure 9.** Excess area analysis ( $A^E$ ) of phospholipid/KL<sub>4</sub> (96:4) monolayers at 25 °C: (a) DPPC/KL<sub>4</sub>; and (b) POPG/KL<sub>4</sub>. The dotted line at  $A^E = 0$  Å<sup>2</sup>/molecule represents ideal mixing. The maximum error in  $A_m$  was no more than  $\pm 0.3$  Å<sup>2</sup>/molecule.

proposed earlier.<sup>13,23,24,37–39</sup> This thermodynamically favorable and preferential electrostatic interaction with anionic PG lipids has been observed to occur *in situ* in DPPC/DPPG lung surfactant protein–phospholipid monolayers.<sup>40</sup> Moreover, favorable cationic–anionic electrostatic interactions

between the cationic lysine amino acids and the anionic PG polar headgroup can effectively “shield” the anionic charge on adjacent PG molecules, thereby promoting closest molecular packing in the monolayer state. This is further reflected in looking at the ternary system of DPPC/POPG/KL<sub>4</sub>, where the value of the equilibrium monolayer collapse surface pressure was significantly increased from a value of 28 to 44 mN/m, and the value of  $\pi_e$  was effectively increased from less than 0.2 mN/m (indicative of a monolayer in the gaseous phase)<sup>6,9</sup> to 45 mN/m. This is further supported by the findings by others that polypeptides consisting of

(37) Cochrane, C.; Revak, S. Protein-Phospholipid Interactions of Pulmonary Surfactant. *Chest* **1994**, *105*, 57S–62S.

(38) Cochrane, C. G.; Revak, S. D.; Merritt, T. A.; Heldt, G. P.; Hallman, M.; Cunningham, M. D. The Efficacy and Safety of KL4-Surfactant in Preterm Infants with Respiratory Distress Syndrome. *Am. J. Respir. Care Med.* **1996**, *153*, 404–410.

(39) Revak, S. D.; Merritt, T. A.; Cochrane, C. G.; Heldt, G. P.; Alberts, M. S.; Anderson, D. W.; Efficacy of Synthetic Peptide-Containing Surfactant in the Treatment of Respiratory Distress Syndrome in Preterm Infant Rhesus Monkeys. *Pediatr. Res.* **1996**, *39*, 715–724.

(40) Brockman, J. M.; Wang, Z.; Notter, R. H.; Dluhy, R. A. Effect of Hydrophobic Surfactant Proteins SP-B and SP-C on Binary phospholipid monolayers II. Infrared external reflectance-absorption spectroscopy. *Biophys. J.* **2003**, *84*, 326–340.

polylysine induce phase separation of lecithin/phosphatidylcholine mixtures.<sup>41</sup> It has been suggested in the literature that KL heteropoly peptide derivatives may form complexes with PC lipids, depending on whether the amphiphilic heteropoly peptide exists in the  $\alpha$ -helix or  $\beta$ -sheet conformations.<sup>42</sup>

To better understand the KL<sub>4</sub> system itself and why it might give rise to such effects on phospholipids, a series of experiments (under equilibrium conditions) focused on the properties of KL<sub>4</sub> cationic hydrophobic surface-active heteropoly peptide alone were carried out, as reported in the Results. It has been shown by others that bulk homopolypeptides of poly-L-lysine and poly-L-leucine can form both the  $\alpha$ -helix or  $\beta$ -sheet conformations in solution depending on conditions, such as the type of solvent, ionic strength, and temperature.<sup>43–46</sup> It has also been shown in the literature that copolypeptides, specifically the heteropoly peptide poly-L-(Lys-Leu-Lys-Leu) can form  $\beta$ -sheet and  $\beta$ -turns in D<sub>2</sub>O solvent.<sup>47</sup> Hence, it is not surprising that KL<sub>4</sub> appears to have a well-defined secondary structure conformation in the solid, solution, and monolayer states. Specifically, the powder X-ray diffractograms seem to indicate that KL<sub>4</sub> in the solid state has  $\beta$ -sheet secondary structure, as deduced from the peak at 19  $2\theta$  and the shoulder at 23.5  $2\theta$ , which is characteristic of this conformation.<sup>31</sup> The peak at about 7  $2\theta$  seems to indicate the presence of an  $\alpha$ -helix (first diffractogram Figure 1a), whereas on the second diffractogram (Figure 1b) the peak resembles that of a  $\beta$ -sheet conformation, as described by Katakai et al.<sup>31</sup> Hence, it appears that KL<sub>4</sub> in the solid state has mainly  $\beta$ -sheet secondary structure, and perhaps some  $\alpha$ -helix. This was confirmed by hot-stage microscopy where birefringence under cross-polarizers was observed which is characteristic of solids having a combination of molecular disorder and order, particularly in surface-active solid-state and liquid crystalline materials.

Using energy minimization techniques in molecular modeling (ChemSite Pro Software; Molecular Modeling Pro Software), it can be further shown (Figure 10) that both the  $\alpha$ -helix and  $\beta$ -sheet secondary structure conformations are

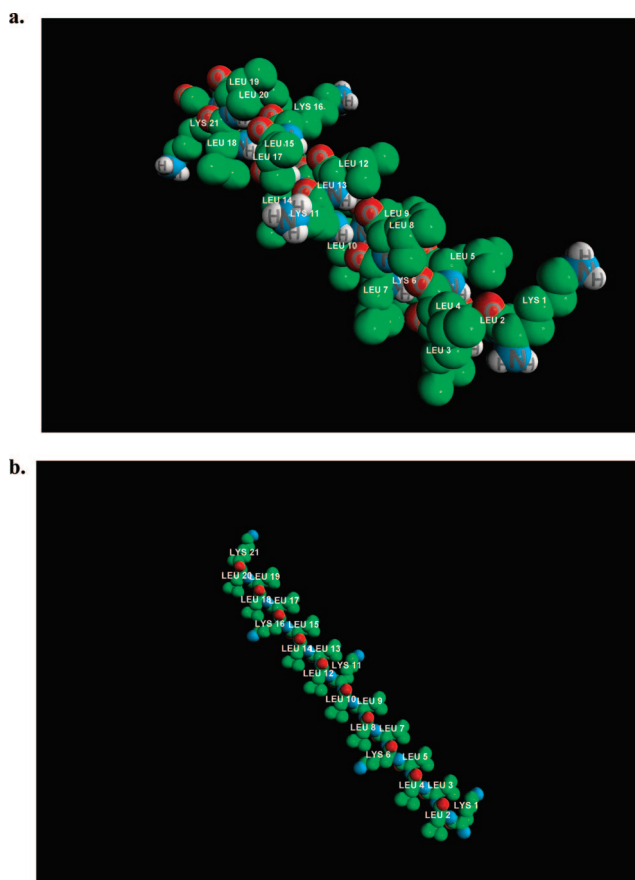


**Figure 10.** Molecular modeling of the secondary structures of KL<sub>4</sub>: (a)  $\alpha$ -helix and (b)  $\beta$ -sheet.

thermodynamically stable, and, hence, possible. This is also in excellent agreement with unpublished molecular modeling using Insight II software (private communication, N. Williams, R. W. Pharmaceutical Research Institute). Calculations from Figure 10 for the  $\alpha$ -helix structure (Figure 10a) reveal that the distance,  $d$ , from lysine 1 to lysine 21 is 33.29 Å, whereas  $\beta$ -sheet (Figure 10b) calculations show that the  $d$  is 71.26 Å. Going back to the KL<sub>4</sub> monolayer isotherm, if the point of lift-off is the point where molecular interactions just begin to be “felt” by individual KL<sub>4</sub> molecules, then this two-dimensional “molecular zone” that one KL<sub>4</sub> molecule “effectively” occupies or “feels” could be described in terms of a circumference,  $c$ , of a circle ( $c = 2\pi r$ ), where the radius of this “molecular circle” at lift-off,  $r$ , is  $d$ , i.e. the distance from lysine 1 to lysine 21. Using this assumption, some calculations can be made in order to better discern what secondary structure KL<sub>4</sub> has when it is confined to two dimensions, as a monolayer at the air–water interface. For  $\alpha$ -helix KL<sub>4</sub>,  $r$  is 33.29 Å, and the predicted area at lift-off is 209.17 Å<sup>2</sup>/KL<sub>4</sub> molecule. For  $\beta$ -sheet KL<sub>4</sub>,  $r$  is 71.26 Å, and the area at lift-off for this conformation is predicted to be 447.74 Å<sup>2</sup>/KL<sub>4</sub> molecule. Going back to the KL<sub>4</sub> monolayer isotherm at 25 °C, lift-off can be seen to occur around 450 Å<sup>2</sup>/KL<sub>4</sub> molecule, which is in very close agreement with the predicted  $\beta$ -sheet value of 447.74 Å<sup>2</sup>/KL<sub>4</sub> molecule. Examining the KL<sub>4</sub> monolayer isotherm, it can be clearly seen that nowhere along the isotherm does

- (41) Mittler-Neher, S.; Knoll, W. Phase Separation in Bimolecular Mixed Lipid Membranes Induced by Polylysine. *Biochem. Biophys. Res. Commun.* **1989**, 162, 124–129.
- (42) Maget-Dana, R.; Lelievre, D. Comparative interaction of  $\alpha$ -helical and  $\beta$ -sheet amphiphilic isopeptides with phospholipid monolayers. *Biopolymers* **2001**, 59, 1–10.
- (43) Greenfield, N.; et al. *Biochemistry* **1967**, 6, 1630.
- (44) Greenfield, N.; Fasman, G. D. Computed circular dichroism spectra for the evaluation of protein conformation. *Biochemistry* **1969**, 8, 4108–4116.
- (45) Sarkar, P. K.; Doty, P. *Proc. Natl. Acad. Sci. U.S.A.* **1966**, 55, 981–989.
- (46) Townsend, R.; Kumosinski, T.; Timasheff, S. N.; Fasman, G. D.; Davidson, B. *Biochem. Biophys. Res. Commun.* **1966**, 23, 163–169.
- (47) Brahms, S.; Brahms, J.; Spach, G.; Brack, A. Identification of  $\beta$ -turns and unordered conformations in polypeptide chains by vacuum ultraviolet circular dichroism. *Proc. Natl. Acad. Sci. U.S.A.* **1977**, 74, 3208–3212.



$A_m$  come close to the predicted  $\alpha$ -helix value of 209.17 Å<sup>2</sup>/KL<sub>4</sub> molecule, not even at monolayer collapse,  $A_c$ .

One may ask what are the important structural features of the  $\alpha$ -helix and  $\beta$ -sheet structures, and what role may these critical structural features play for a cationic hydrophobic surface-active heteropolypeptide, such as KL<sub>4</sub>, when confined to two-dimensions at an interface. As presented by Damodaran, proteins at an interface (as opposed as to when in solution) appear to lose  $\alpha$ -helix structure and gain  $\beta$ -sheet and random structures.<sup>22</sup> This appears to be the case with the heteropolypeptide, KL<sub>4</sub>. As discussed above, molecular modeling quantitatively indicates that the distance from lysine 1 to lysine 21 is quite different for both conformations. The  $\beta$ -sheet structure can incorporate the side chains (as well as the peptide backbone) in hydrogen-bonding leading to favorable hydrophobic interactions between hydrophobic residues, thereby shielding these residues. Consequently, the  $\beta$ -sheet conformation of KL<sub>4</sub> is longer (molecular model:  $d = 71.26$  Å) and more flexible (three amino acids per turn) than its  $\alpha$ -helix conformation. Contrastingly, the  $\alpha$ -helix conformation of KL<sub>4</sub> is more compact (molecular model:  $d = 33.29$  Å) as only the peptide backbone (not the side chains) is involved in hydrogen-bonding at every  $(n+4)$ th amino acid, i.e., 3.6 amino acids per turn. Hence, the side chains must be projected outward and exposed. Therefore, it is reasonable that the conformation of KL<sub>4</sub> confined to two dimensions, such as the air–water interface, where polarity (aqueous bulk phase) and hydrophobicity (air) are both present, may have a restricted conformation (“fixed conformation”) where the hydrophobic residues are shielded (facilitated by the  $\beta$ -sheet conformation) from the aqueous surface; by facing toward the air and away from the water while maximizing favorable leucine–leucine hydrophobic interactions, van der Waals interactions, and lysine–water polar and hydrogen-bonding interactions. Hence, it follows that the conformation in solution (three dimensions) or in the solid-state (three dimensions) can conceivably be different than that at an interface (two dimensions), as has been demonstrated with water-soluble proteins in solution and at the air–water interface.<sup>22</sup> Hence, interfacial conformational restructuring of polypeptides and proteins occurs. KL<sub>4</sub> in solution CD spectra indicates that KL<sub>4</sub> is in the  $\alpha$ -helix conformation (positive peaks between 190 and 200 nm, negative peak at 207–208 nm) in good agreement with unpublished results (private communication, N. Williams, R. W. Pharmaceutical Research Institute) and with the solution conformation of SP-B,<sup>48–50</sup> KL derivatives<sup>51</sup> and lysine-containing peptides.<sup>52</sup>

Quantitative analysis of the amount of the various secondary structures seen in the solution and surface CD spectra of KL<sub>4</sub> monolayers at various surface pressures was carried out using CDESTIMA software,<sup>53</sup> as applied to surface CD spectra by others.<sup>22</sup> This software can be a *guide* in *estimating* the amount of various secondary structures at a surface; however, the database from which these surface CD quantifications are made is obtained from the CD spectra of 15 globular proteins with known secondary structures in

solution (i.e., solution CD). Positive peaks at 195 nm and just below 200 nm and negative peaks at 210–220 nm are characteristic of  $\beta$ -sheets. Positive peaks at 200–205 nm and a negative peak at 225 nm are characteristic of a  $\beta$ -turn. The positive peak at 218 nm and the negative peak just below 200 nm are characteristic of random structure. Estimation of the solution CD spectra of KL<sub>4</sub> indicates 30%  $\alpha$ -helix, 0%  $\beta$ -sheet, 20%  $\beta$ -turns, and 50% random conformations. Estimation of the CD spectra of the KL<sub>4</sub> monolayers at all surface pressures studied indicates that, by using a first-order estimation, 85%  $\beta$ -sheets and 15% random structures exist. Second-order estimation indicates 82%  $\beta$ -sheet, 17.5% random, and 0.5%  $\beta$ -turn structures. Indeed, the air–water interface appears to confine KL<sub>4</sub> into a conformation that allows the hydrophobic leucine residues to be shielded away from water due to the hydrophobic effect, while maximizing lysine interactions with water (polar–polar and hydrogen-bonding interactions), by resorting to the  $\beta$ -sheet conformation. This conformation appears to be the predominant conformation seen in both the solid-state and monolayer state.

When mixed with DPPC and POPG, KL<sub>4</sub> exhibits secondary conformations. Since the intensities of the KL<sub>4</sub> CD signal were smaller (as would be expected for a binary mixture), CDESTIMA was not used to quantify the various conformations. The CD spectra of KL<sub>4</sub> in DPPC monolayers indicate that KL<sub>4</sub> exists predominantly in the  $\beta$ -sheet and some random conformations, similar to KL<sub>4</sub> monolayers in the absence of DPPC. This is in good agreement with the surface studies, where DPPC and KL<sub>4</sub> appear to be phase-separated. *In situ* IRRAS of DPPC/KL<sub>4</sub> monolayers (at a different molar composition) on D<sub>2</sub>O subphase under time-dependent (dynamic) compression showed that the  $\beta$ -sheet secondary structure of KL<sub>4</sub> was detected.<sup>16</sup> When mixed with POPG, however, the conformation of KL<sub>4</sub> appears to favor an increase in aperiodic structure with some  $\beta$ -sheet structure. This also agrees with the surface studies where POPG and

- (48) Kang, J.; Lee, M.; Kim, K.; Hahm, K.-S. The Relationships Between Biophysical Activity and the Secondary Structure of Synthetic Peptides From the Pulmonary Surfactant Protein SP-B. *Biochem. Mol. Biol. Int.* **1996**, *40*, 617–627.
- (49) Andersson, M.; Curstedt, T.; Jorvall, H.; Johansson, J. An Amphipathic Helical Motif Common to Tumourolytic Polypeptide NK-Lysin and Pulmonary Surfactant Polypeptide SP-B. *FEBS Lett.* **1995**, *362*, 328–332.
- (50) Cruz, A.; Casals, C.; Perez-Gil, J. Conformational Flexibility of Pulmonary Surfactant Proteins SP-B and SP-C, Studied in Aqueous Organic Solvents. *Biochim. Biophys. Acta* **1995**, *1255*, 68–76.
- (51) DeGrado, W. F.; Lear, J. D. Induction of peptide conformation at apolar/water interfaces. 1. A Study with model peptides of defined hydrophobic periodicity. *J. Am. Chem. Soc.* **1985**, *107*, 7684–7689.
- (52) Vogt, B.; Ducarme, P.; Schinzel, S.; Brasseur, R.; Bechinger, B. The topology of lysine-containing amphipathic peptides in bilayers by circular dichroism, solid-state NMR, and molecular modeling. *Biophys. J.* **2000**, *79*, 2644–2656.
- (53) Chang, C. T.; Wu, C. S. C.; Yang, J. T. Circular Dichroic Analysis of Protein Conformation: Inclusion of the  $\beta$ -Turns. *Anal. Biochem.* **1978**, *91*, 3–31.

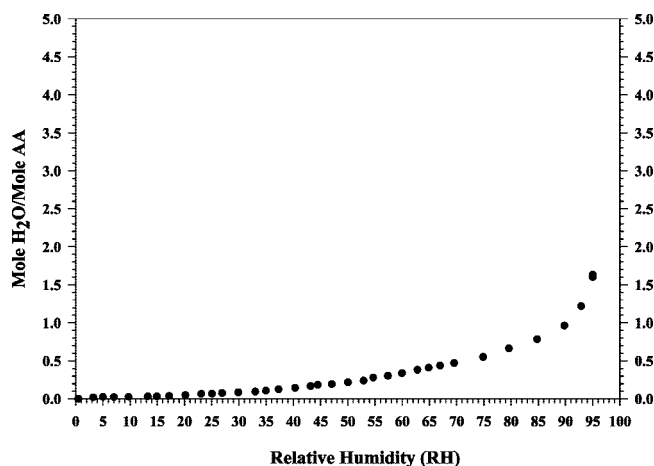


**Figure 11.** Water vapor sorption per mole amino acid isotherm of KL<sub>4</sub> at 25 °C following preconditioning at 25 °C (●).

KL<sub>4</sub> have net attractive interactions through favorable electrostatic interactions, which expectedly affect the secondary structure of KL<sub>4</sub> at the air–water interface through interfacial conformational restructuring of KL<sub>4</sub> when confined to two-dimensions.

Water molecules play a critical role in the secondary structural conformations of polypeptides and proteins, which, in turn, can affect protein function. The study of water vapor sorption behavior of proteins in the solid-state dates back several decades,<sup>54–56</sup> and the effect of the level of hydration on biomacromolecular structure and stability of proteins in the solid state has been reviewed.<sup>57</sup> It has been shown, for proteins, that the primary water sorption sites do not have identical degrees of hydrophilicity.<sup>56</sup> Specifically, just as the level of hydration affects inter- and intrabilayer interactions and bilayer structure of phospholipids in the solid-state,<sup>25</sup> water molecules affect polypeptide and protein structures. Specifically, water molecules can facilitate and optimize hydrogen bonding between various residues in polypeptides and proteins by directly interacting with polar residues and/or forming a hydrogen-bonding bridge network between nonpolar residues. Additionally, sorbed water molecules can form a hydrogen bond network with the peptide carboxyl and imido groups.<sup>54</sup> To gain a better perspective of the hydration characteristics of KL<sub>4</sub>, which in turn gives valuable insight into its secondary structure when confined in two-dimensions at an air–water interface, an analysis of Figure 2 can be carried out. Shown in Figure 11 is the equilibrium

water vapor sorption per amino acid isotherm of KL<sub>4</sub> which shows that approximately 1.6 mol of water per amino acid is present at 95% RH, approaching a full hydration environment. It appears that, despite the presence of five cationic lysine residues, which would be expected (based on polarity) to take up a significant amount of water, the highly hydrophobic character of KL<sub>4</sub> (imparted by the leucine residues) appears to dominate the overall water vapor sorption profile of KL<sub>4</sub> as demonstrated by minimal water vapor uptake even at very high water levels. Using the Kuntz estimation of 4.5 molecules of water sorbed per Lysine amino acid and 1 molecule of water per leucine amino acid,<sup>55</sup> it can be estimated that 38.5 water molecules per KL<sub>4</sub> molecules would be *expected* to be bound at full hydration. This *predicts* that approximately 1.8 molecules of water per amino acid in KL<sub>4</sub> are bound, which is in excellent agreement with the *experimental* value of approximately 1.6 water molecules per amino acid. This value is much closer to the value of leucine than to lysine.

As demonstrated in this study and revealed for the first time under thermodynamic equilibrium time-independent conditions, the implications for effective pulmonary surfactant delivery are several and significant. Thermodynamic implications for pulmonary surfactant delivery and the surface chemical characteristics necessary are the following: (1) a high monolayer collapse surface pressure with an equilibrium value of  $\pi_c \sim 45$  mN/m; (2) spontaneous and instantaneous bilayer spreading with an equilibrium value of  $\pi_c \sim 45$  mN/m; (3) significant monolayer expansion at higher molecular areas in the LE phase; (4) adequate monolayer condensation at lower molecular areas in the LC phase; and (5) the hydrophobic effect, interfacial polar interactions, and interfacial electrostatic interactions can lead to interfacial unfolding and interfacial conformational restructuring of biomacromolecules, potentially affecting both the functionality of pulmonary surfactant and the therapeutic biomacromolecule.

## Conclusions

In a three-dimensional (bulk) state, solid-state KL<sub>4</sub> exhibits a distinct secondary structure conformation (predominantly  $\beta$ -sheet and, perhaps, some  $\alpha$ -helix), whereas KL<sub>4</sub> in solution appears to exist in the  $\alpha$ -helix secondary structure. KL<sub>4</sub> forms a stable, insoluble monolayer, where the  $\beta$ -sheet and aperiodic secondary structures appear to be the predominant conformations of KL<sub>4</sub> when confined to two dimensions at the air–water interface, indicative of interfacial restructuring of the heteropolypeptide conformation. These conformations, when KL<sub>4</sub> is confined to two dimensions, appear to provide structural flexibility. Interfacial conformational restructuring, arising from structural flexibility, maximizes favorable cationic lysine–water (polar–polar and hydrogen-bonding) interactions and favorable leucine–leucine hydrophobic and van der Waals interactions; while effectively “shielding” the hydrophobic leucine residues away from water which is thermodynamically favorable due to the hydrophobic effect. KL<sub>4</sub> appears to have a negligible effect on zwitterionic DPPC due to phase-separation of DPPC

(54) Pauling, L. The Adsorption of Water By Proteins. *J. Am. Chem. Soc.* **1945**, 67, 555–557.

(55) Kuntz, I. D. Hydration of Macromolecules. III. Hydration of Polypeptides. IV. Polypeptide Conformation in Frozen Solutions. *J. Am. Chem. Soc.* **1971**, 93, 514–518.

(56) Leeder, J. D.; Watt, I. C. The Stoichiometry of Water Sorption by Proteins. *J. Colloid Interface Sci.* **1974**, 48, 339–344.

(57) Hill, J. J.; Shalae, E. Y.; Zografi, G. Thermodynamic and dynamic factors involved in the stability of native protein structure in amorphous solids in relation to levels of hydration. *J. Pharm. Sci.* **2005**, 94, 1636–1667.

and KL<sub>4</sub> in both the bilayer and monolayer states. This may be attributed to negligible interactions of cationic KL<sub>4</sub> with the zwitterionic PC polar headgroup. KL<sub>4</sub> in DPPC/KL<sub>4</sub> monolayers appears to retain its  $\beta$ -sheet and aperiodic secondary structures, consistent with complete phase separation (ideal mixing phase behavior) of DPPC and KL<sub>4</sub> in bilayers and monolayers resulting in the attainment of a maximal surface pressure (from both the bilayer and monolayer states) and a highly condensed monolayer. Conversely, KL<sub>4</sub> in POPG/KL<sub>4</sub> monolayers appears to have an increase in aperiodic secondary structures, due to interfacial restructuring of the conformation to maximize these favorable attractive electrostatic interactions, consistent with negative deviations from ideality (nonideal mixing phase behavior) observed in the condensing of POPG/KL<sub>4</sub> monolayers, and the lack of inhibition of KL<sub>4</sub> on maximal POPG bilayer spreading. In DPPC/POPG, KL<sub>4</sub> promotes maximal spreading, maximal surface tension reduction, and enhanced condensation of the otherwise miscible DPPC/POPG mixture through promoting phase separation of DPPC and POPG. This may promote the important lung surfactant functionality of the necessary increase in both the bilayer spreading and monolayer collapse surface pressures of the binary mixture in the presence of KL<sub>4</sub>.

**Acknowledgment.** Generous financial support from a two-year Pre-Doctoral Fellowship in Pharmaceutics from the American Foundation for Pharmaceutical Education (AFPE) and a two-year Advanced Pre-Doctoral Fellowship in Pharmaceutics from the Pharmaceutical Manufacturers and Researchers of America (PhRMA) Foundation is gratefully acknowledged. Dr. Gary Case at the University of Wisconsin—Madison Biotechnology Center is gratefully acknowledged for his expertise in the synthesis and high purification of KL<sub>4</sub>. Professor Juan DePablo (U.W.—Madison College of Chemical and Biological Engineering) is thanked for sharing his X-ray diffractometer with us, and Dr. Kieran Crowley is thanked for his assistance with XRPD. At Purdue University, Professor Jeffrey Bolin (Dept. of Biological Sciences), and Professors Ken Morris and Joseph Stowell at the School of Pharmacy and Pharmaceutical Sciences are acknowledged for having been very helpful in polypeptide X-ray analysis. Professor Hyuk Yu (U.W.—Madison Dept. of Chemistry) is thanked for his helpful suggestions.

MP700123P